Reprinted from SPIE vol. 1071-Optical Sensors and Electronic Photography

Image Signal Modulation and Noise Characteristics of Charge-Coupled Device Imagers

Peter D. Burns

Commercial and Information Systems Group Research Laboratories
Eastman Kodak Company, Rochester, New York 14653-5719

Abstract

A physical model is used to describe the image modulation and noise characteristics of charge-coupled device (CCD) imagers. The model includes the effects of photon absorption, charge generation and collection, and signal quantization. The imaging characteristics are presented in terms of the MTF and Wiener, or noise power, spectrum. A computed example illustrates the use of the model.

1. Introduction

The improvements in performance and reliability of charge-coupled device (CCD) sensors have led to their wide application in electronic imaging systems. These systems often employ several technologies to detect, process and display the image information and the characteristics of any subsystem can limit system imaging performance. A consistent systematic description of signal modulation and noise degradation is valuable when identifying limitations to image quality. Such an analysis can be used in system development to set imaging requirements and also in the simulation of imaging performance. In particular, signal-to-noise ratio techniques aid in the comparison of competing technologies employing different imaging mechanisms, and in the evaluation of ultimate (e.g., quantum-limited) performance.

The analysis of electro-optical systems in this way requires a description of the imaging performance of each element in the signal chain. System optimization can then be attempted, given specific criteria such as information capacity or fidelity.[1-4] Improvements in solid state detectors have come about by identifying specific internal mechanisms that limit performance. The aim here is to describe the signal modulation and noise characteristics of CCD imagers in terms of the various parameters associated with charge generation, collection and readout. The emphasis will be on their contribution to system imaging characteristics for visible light applications.

A CCD imager consists of a detector, CCD shift register and amplifier.[5,6] We will also consider the quantization step but not the effect of scanning optics. The input exposure is detected and converted to a sampled, quantized record before it is stored or transmitted. In general, the effect of the various signal processing steps on the final image is not isotropic and depends on the specific architecture (e.g., area or linear array type, pixel size). We will express the imaging characteristics (i.e., transfer functions and noise sources) in terms of the input image dimensions, given a particular imaging application. The device will be oriented so x is along the CCD array. Two types of noise sources will be considered: those independent of the signal, and those that are a function of its mean value. Aliasing errors,[7] which are also dependent on the image autocorrelation, are not addressed.

Although CCD cameras vary in the materials used, fabrication and architecture, several common signal transformations can be identified.[5,6] Figure 1 shows a functional block diagram of a CCD sensor in the focal plane of an optical system and its associated electronics. Incident photons are detected in the photosensitive layer simultaneously at each photosite (pixel) location across the detector. The energy released by the absorbed photons generates electron-hole pairs. The electrons then migrate to potential wells in the device so that the collected charge represents the signal integrated over each photosite. This charge, collected during a fixed time interval, is then transferred from the potential wells through a shift register to the readout node. The final step is the readout of the charge packets, analog amplification and quantization of the signal.

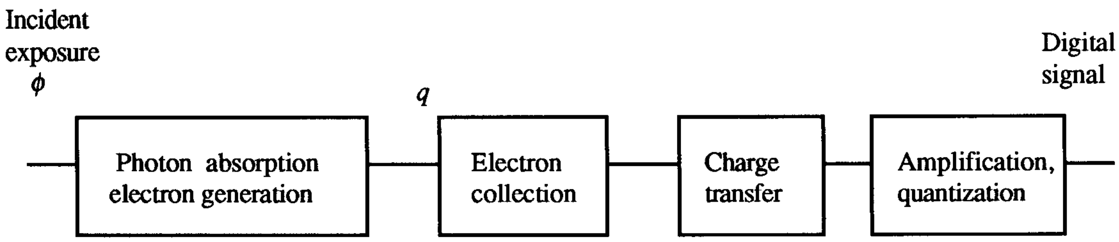

Figure 1. Functional diagram for CCD imager.

2. Model

As each step of the imaging system is examined, the signal and noise characteristics will be described in terms of the resulting MTF and Wiener, or noise power, spectrum. The application of the MTF to describe the signal transformations in solid state sensors is well established.[5,6,8-10] The noise power spectrum[11,12] is the two-dimensional spectral density for a wide sense-stationary stochastic process (e.g., number of electrons/pixel). It represents the decomposition of the variance over spatial frequency. In order to provide an absolute noise measure, this can be expressed in units of variance·area. The noise power spectrum for the case of a uniform uncorrelated photon exposure will now be analyzed at various steps in the signal path. For a uniform exposure of μ_ϕ photons/area the fluctuations are governed by Poisson statistics and therefore the variance is

$$\sigma_\phi^2 = \mu_\phi \ .$$

The chance of a photon being absorbed by the photosensitive material depends on both the optical surface characteristics and absorption properties of silicon. Since we are only considering visible light, it is assumed that each absorbed photon generates a single electron-hole pair.[6] A fraction of the generated electrons are lost. The absorption of light of wavelength λ, generation and loss of charge is described by the absolute quantum efficiency, $\eta(\lambda)$, which is the probability that an incident photon generates a collected electron. This can be described as the multiplication of the quantum exposure by a binomial random variable with mean, η. No scattering is associated with the absorption and therefore there is no resulting degradation of signal modulation. We will associate any scattering prior to absorption with charge diffusion, which follows. If η is assumed constant, the image noise remains uncorrelated but with reduced variance

$$\sigma_q^2 = \mu_q = \eta\, \mu_\phi \ . \tag{1}$$

Not all of the charge generated by incident illumination at a given pixel is collected and contributes to the signal charge at that pixel. The diffusion of charge in the sensor remains a serious source of image degradation. Charge diffusion causes the signal charge generated within a pixel boundary to be collected at neighboring pixels. Seib[8] developed diffusion expressions for front- and backside-illuminated CCDs based on a model by Crowell and Labuda.[13] Blouke and Robinson[9] addressed the case of a frontside-illuminated device with an epitaxial layer aimed at reducing charge diffusion. More recently, Monte Carlo simulation techniques have been used to model diffusion in more complicated devices.[14] For our purposes, charge diffusion will be viewed as a stochastic scattering process. The probability density function associated with the scattering of electrons from point of generation to that of collection becomes a point spread function (psf). The Fourier transform of the psf is the corresponding MTF, $H_d(u, v)$, where u and v are the spatial frequency coordinates. Note that merely scattering spatially uncorrelated electrons does *not* change the noise power spectrum. So, although the image signal modulation is reduced, the noise power spectrum remains flat (white).[15]

It is not possible to measure the diffusion MTF without including the MTF due to charge integration which, for a rectangular photosite is

$$H_i(u,v) = \frac{\sin(2\pi u\,\Delta x)}{2\pi u\,\Delta x}\,\frac{\sin(2\pi v \Delta y)}{2\pi v \Delta y} \tag{2}$$

where Δx and Δy are the dimensions of the active pixel area. Charge integration also represents sampling of the continuous charge density, and a more complete treatment would include aliasing artifacts introduced here.[6] The modulation transfer functions combine[9] so the MTF associated with diffusion and integration is

$$H_{d\text{-}i}(u,v) = H_d(u,v)\, H_i(u,v) \quad . \tag{3}$$

The integrated charge will have a mean and variance given by

$$\begin{aligned} \mu_i &= \Delta x\ \Delta y\ \mu_\phi \quad , \\ \sigma_i^2 &= \Delta x\ \Delta y\ \mu_\phi \end{aligned} \tag{4}$$

since the input exposure was expressed as charge/area, and the integrated charge is in terms of charge/pixel. The integrated pixel charge is Poisson distributed since each is the sum of independent Poisson random variables.[16] The spectrum shape remains unchanged since the pixel integration is over nonoverlapping regions containing the uncorrelated charge fluctuations so

$$S_i(u,v) = \mu_i \qquad \text{electrons}^2 \cdot \text{pixel} \quad . \tag{5}$$

The integrated charge is now transferred from the sensor to the charge-coupled device array. The CCD transfers the charge packet repeatedly over the length of the device to the output amplifier. At each transfer a small fraction, ε, of the signal charge is left behind and therefore is added to the next pixel charge. This introduces a nonstationary blurring of the image which, for a simple readout scheme, can be approximated by the MTF[5,10]

$$H_t(u) \cong \exp(-N\varepsilon(\ 1 - \cos(2\pi uX)\ ) \tag{6}$$

where N is the total number of transfers and X is the effective image sampling interval.

The loss of charge also represents a source of image noise. If the charge lost during each transfer can be described, as above, as a fixed fraction, then the corresponding variance is[17]

$$\sigma_\varepsilon^2 = 4\varepsilon^2 \mu_i\, N \quad . \tag{7}$$

The noise power spectrum for the transferred signal is

$$S_t(u,v) = S_i(u,v)\ H_t^2(u,\ v) + S_\varepsilon\,(u,v) \quad , \tag{8}$$

where S_ε is the component due to charge transfer inefficiency. Recent improvements, including the use of buried channel CCDs, have increased the charge transfer efficiency, making this a minor source of image degradation for many devices.

So far the fluctuations in the uniform image signal are due to the intrinsic detection, collection and transfer of quantum exposure fluctuations. The variance of this shot noise is proportional to the mean signal. Two other sources of noise are important: fixed pattern noise and read noise. Fixed pattern noise results from pixel-to-pixel sensitivity variations in the device, i.e., variations in η and volts/electron for each pixel. Recently,[17,18] several sources of fixed pattern noise have been identified and reduced. The effect of fixed pattern noise can also be reduced by calibration and post processing. The residual uncompensated component is read noise.

The read noise is independent of the mean signal and is a result of several sources[20] including background noise,[5] reset noise[21] and output amplifier noise.[6,16] This is treated as a combined uncorrelated noise source, with zero mean and variance σ_r^2.

The on-chip output amplifier contributes two components to the read noise, an uncorrelated white noise and a source with a 1/f spectral density. We model the output as in reference 6 as the addition of these two sources followed by a linear filter that includes the response of any correlated double sampling operation[21] and integration of the A/D converter. The MTF from input to amplifier and noise power spectrum at the output of the amplifier are

$$H_{d\text{-}a}(u,v) = H_d(u,v)\, H_i(u,v) H_t(u) H_a(u) \ , \tag{9}$$

$$S_a(u,v) = \{S_t(u,v) + S_r(u,v)\}\, H_a^2(u) \ . \tag{10}$$

The exposure range and number of quantization bits used in the CCD imager depend on the imaging application. They are usually chosen to minimize the visibility of image quantization artifacts. For continuous-tone images and scientific applications this may require more than 8 bits, with the size of each interval being a nonlinear function of input exposure. Here we model the process of quantization as the addition of a zero-mean quantization noise source. Making the usual assumption of a uniform distribution of error about a given quantization interval, the variance is given by[2]

$$\sigma_b^2(\mu_\phi) = \frac{\Delta q^2(\mu_\phi)}{12} \qquad \text{electrons}^2 \ ,$$

where $\Delta q(\mu_Q)$ is the quantization interval written as a function of average input signal. The corresponding noise power spectrum is

$$S_b(\mu_\phi,u,v) = \frac{\Delta q^2(\mu_\phi)}{12} \qquad \text{electrons}^2 \text{ pixel} \ , \tag{11}$$

For the special case of uniform quantization intervals

$$S_b(u,v) = \frac{q^2{max}}{12 \ 2^{2b}} \qquad \text{electrons}^2\text{pixel} \ , \tag{12}$$

where q_{max} is the maximum pixel charge, and b is the number of bits used.

Each step in the signal chain has now been addressed and is shown schematically in Figure 2. The system MTF is the product of each component MTF from equations (2), (3), (6) and (9):

$$MTF(u,v) = H_d(u,v) H_i(u,v) H_t(u) H_a(u) \ .$$

The output Wiener spectrum, from equations (5), (8), (10) and (11) is

$$S(u,v) = \left\{\mu_i \, H_t^2(u) + S_\varepsilon\,(u,v) + S_r\,(u,v)\right\} H_a^2(u) + S_b(u,v) \quad . \tag{13}$$

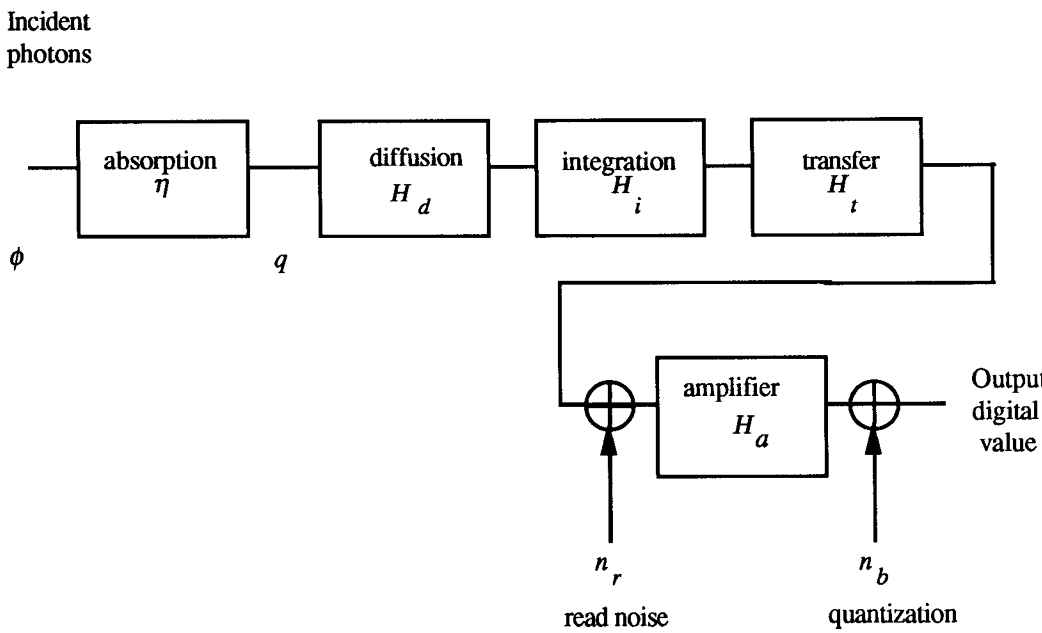

Figure 2. Schematic diagram of CCD imager model.

3. Computed Example

Consider a linear array CCD image to be used for scanning hardcopy images. The manufacturer specifies that the maximum, or full well, charge is 10^5 electrons and the dynamic range (q_{max}/RMS pixel read noise) is 1500. Since the image noise associated with input document granularity is often expressed in terms of its Wiener spectrum, we are interested in the apparent spectrum due to the CCD imager when it scans a uniform area. The signal is quantized using 8 bits. For this example we will assume that the charge transfer efficiency is high (H_t = 1. and S_ε = 0.), and amplifier 1/f noise is negligible when compared to other read noise sources.

From equation (13) we only need the amplifier MTF, which we will assume to be described by a simple low-pass filter

$$H_a(u) = \frac{1}{1 + \frac{u}{7}} \quad ,$$

where u is in cy/mm on the input document. An alternative MTF is that derived for correlated double sampling readout, given reference 21. The read noise power spectrum from equation (12) is

$$S_r\,(u,v) = \left(\frac{q_{max}}{DR}\right)^2 H_a^2(u) \tag{14}$$

$$= 4.44 \times 10^3\, H_a^2(u) \quad \text{electrons}^2 \text{ pixel} \;, \tag{15}$$

where DR is the dynamic range. The shot noise power spectrum for a mean charge μ_q is

$$S_q\,(\mu_q\,,u,v) H_a^2(u) = \mu_q\, H_a^2(u) \;\; \text{electrons}^2 \text{ pixel} \;\;. \tag{16}$$

For uniform quantization, from equation (12) the spectrum is

$$S_q = \frac{q_{max}^2}{12\; 2^{16}} = 1.27 \times 10^4 \;\; \text{electrons}^2 \text{ pixel} \;\;.$$

For hardcopy images we need to express the CCD imager noise in terms of reflectance or, more often, optical density. If we require that the imager noise be expressed in terms of reflectance (or transmittance), we first establish that the maximum reflectance, 1.0, corresponds to the saturation charge, q_{max} (this may not always be the case). Dividing each of the noise power spectrum components by $q_{max}{}^2$ therefore expresses them in units of R^2 pixel. These fluctuations can then be expressed in density using the approximation

$$S_{density}(u,v) \cong \frac{(\log_{10} e)^2\, S_{reflectance}(u,v)}{mean\;\; reflectance^2} \;\;. \tag{17}$$

If the noise power spectrum is to be expressed in terms of density^2 μm^2 on the hardcopy input image, as is usually done for photographic prints, then this is given by substituting equations (14), (15) and (16) into (13) and (17)

$$S_a(\mu_q,u,v) = \frac{(\log_{10} e)^2\, \Delta x \Delta y \left\{\left[\mu_i + \left[\frac{q_{max}}{DR}\right]^2\right] H_a^2(v) + \frac{q_{max}^2}{12\;\; 2^{16}}\right\}}{\mu_i{}^2} \quad D^2 \mu m^2 \;\;.$$

Figures 3-5 show the noise power spectrum of the CCD imager as a function of spatial frequency and average density. To plot the function here, the single frequency axis corresponds to u=v. The calculated Wiener spectrum levels are higher than those usually measured for photographic print granularity, but comparable to dry electrophotographic granularity. Film scanning usually requires more than eight bits of quantization, and a CCD imager dynamic range greater than 1500 (i.e., lower read noise levels than in this example).

4. Conclusions

The functional model for a CCD imager provides a way to interpret the imaging performance that is consistent with established metrics for not only photographic but also other electro-optical systems. It facilitates the comparison of detectors and the selection of any CCD device in the context of the subsequent image processing and display tasks to performed.

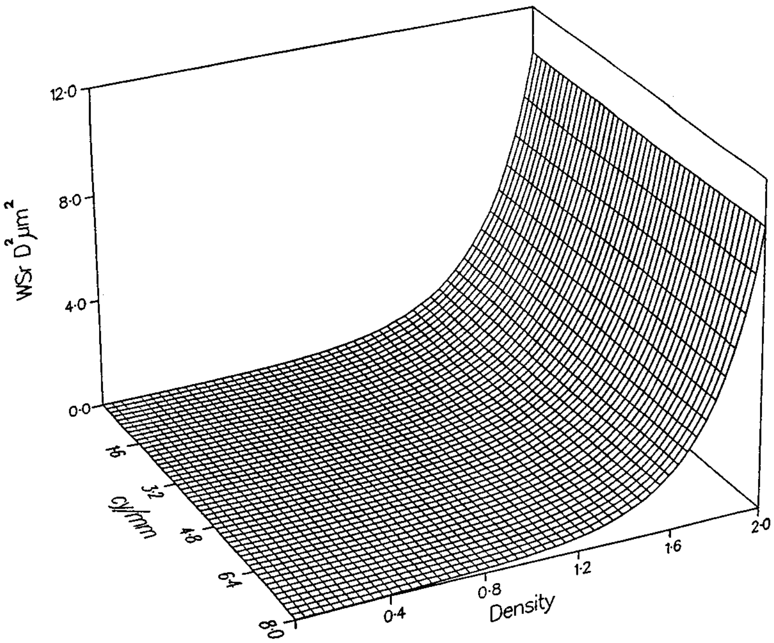

Figure 3. Noise power spectrum of read and shot noise for the computed example.

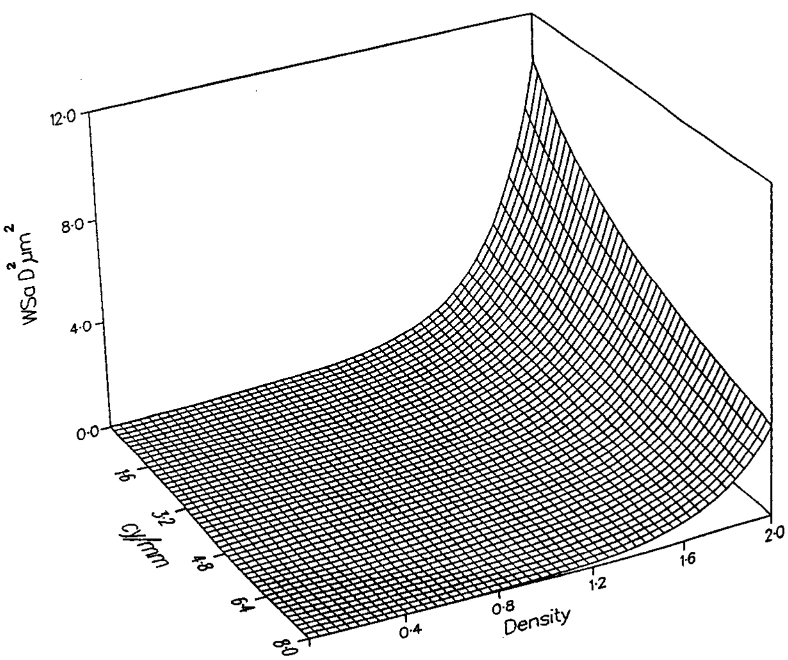

Figure 4. Noise power spectrum for the output of the amplifier.

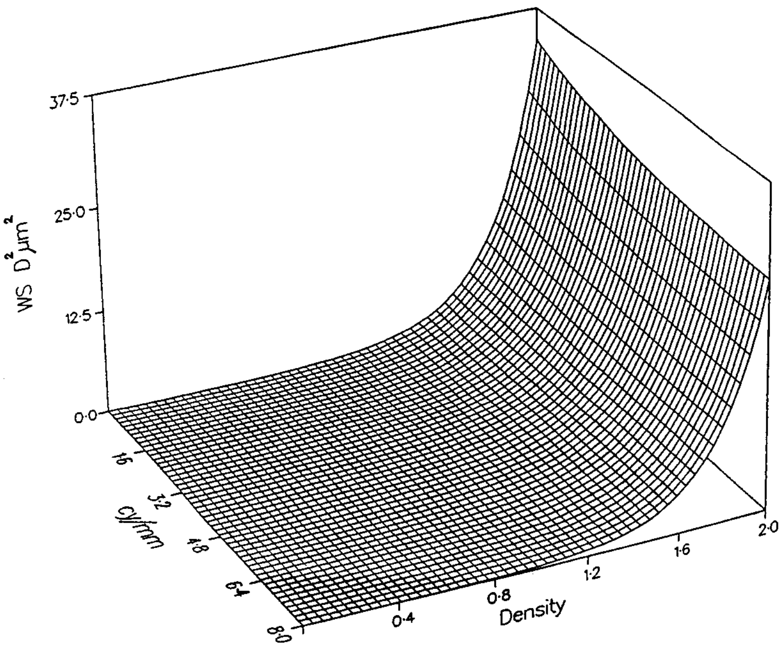

Figure 5. Noise power spectrum for the quantized image (note change of scale).

6. *Acknowledgements*

I thank J. R. Sullivan for his help during many useful discussions regarding the characteristics of CCD imagers, and review of this paper. I am also grateful to T. J. Tredwell for his comments.

7. *References*

1. F. O. Huck, C. L. Fales, N. Halyo and W. Samms, "Image Gathering and Processing: Information and Fidelity," *JOSA/A* 2: 1644-1665 (1985).
2. W. T. Cathey, B. R. Freiden, W. T. Rhodes and C. K. Rushforth, "Image Gathering and Processing for Enhanced Resolution," *JOSA/A* 1: 241-250 (1984).
3. M. E. Dunham and P. G. Sanchez, "Ultimate Sensitivity and Resolution of Phosphor/Fiber/ Charge-Coupled Device System," *Opt. Eng.* 26: 1035-1041 (1987).
4. R. Shaw, "Quality Criteria for Quantized Images," *Proc. SPIE* vol. 901: (1988).
5. D. F. Barbe, "Imaging Devices Using the Charge-Coupled Concept," *Proc. IEEE* 63: 38-67 (1975).
6. J. R. Janesick, T. Elliot, S. Collins, M. M. Blouke and J. Freeman, "Scientific Charge-Coupled Devices," *Opt. Eng.* 26: 692-714 (1987).
7. F. O. Huck and S. K. Park, "Aliasing and Blurring in 2-D Sampled Imagery," *Appl. Opt.* 19: 2174-2181 (1980).
8. D. H. Seib,"Carrier Diffusion Degradation of Modulation Transfer Function in CCD," *IEEE Trans. Electron Devices*, ED-21: 210-217, (1974).
9. M. M. Blouke and D. A. Robinson, "A Method for Improving the Spatial Resolution of Frontside Illuminated CCD's," *IEEE Trans. Electron Devices*, ED-28: 251-256, (1981).
10. H. Herbst and H. J. Pfleiderer," Modulation Transfer Function of Quadrilinear CCD Imager," *Electron. Letters* 12:676-6777 (1976).
11. C. J. Dainty and R. Shaw, *Image Science*, Academic Press, London, 1974, ch.8.

12. G. D. Boreman, "Fourier Spectrum Techniques for Characterization of Spatial Noise in Imaging Arrays," *Opt. Eng.* 26: 985-991 (1987).
13. M. H. Crowell and E. F. Labuda, "The Silicon Diode Array Camera Tube," *Bell Syst. Tech. J*, 48: 1481-1528, (1969).
14. J. P. Lavine, W.-C. Chang, C. N. Anagnostopoulos, B. C. Burkey and E. T. Nelson, "Monte Carlo Simulation of the Photoelectron Crosstalk in Silicon Imaging Devices," *IEEE Trans. Electron Devices*, ED-32: 2087-2090, (1985).
15. M. Rabbani, R. Shaw and R. VanMetter, "Detective Quantum Efficiency of Imaging Systems with Amplifying and Scattering Mechanisms," *JOSA/A* 4: 895-901 (1987).
16. A. Papoulis, *Probability, Random Variables and Stochastic Processes,* McGraw-Hill, New York, (1965), P.214.
17. J. Carnes and W. Kosonocky, "Noise Sources in Charge-Coupled Devices," *RCA Rev.* 33: 327-343 (1972).
18. J. Janesick and T. Elliot, "Spurious Potential Packets and Pixel Nonuniformity in CCDs," in *9th Santa Cruz Workshop in Astronomy and Astrophysics: Instrumentation for Ground Based Optical Astronomy*, Lick Observatory, (1987).
19. K. Orihara and E. Oda, "Generation Mechanism and Elimination of Fixed Pattern Noise in Dual Channel Horizontal-CCD Register Image Sensor," *IEEE Trans Electron Dev.* ED-35: 1846-1850 (1988).
20. T-H. Lee, T. J. Tredwell, B. C. Burkey, C. Anagnostopoulos, J, S. Hayward, T. M. Kelly, R. P. Khosla, D. L. Losee and J. P. Lavine, "A Solid-State Image Sensor for Image Recording at 2000 Frames per Second," *IEEE Trans. Electron. Dev.* ED-19: 1469-1477 (1982).
21. M. H. White, D. R. Lampe, F. C. Blaha and I. Mack, "Characterization of Surface Channel CCD Image Arrays at Low light Levels," *IEEE J. Solid-State Cir*, SC-9: 1-12 (1974).
22. A. V. Oppenheim and R. W. Schafer, *Digital Signal Processing*, Prentice Hall, Engelwood Cliffs, N. J., 1975, pp.409-413.